SUPPLEMENTARY METHODS

Gamma secretase inhibitor and Jag1 treatments. 100 mg/kg DAPT (N-[N-(3,5-Difluorophenacetyl-L-alanyl)]-S-phenylglycine t-Butyl Ester; Sigma or Calbiochem, 565770) or 1-20 mg/kg Compound X (synthesized as described[1] and dissolved in 10% ethanol and 90% corn oil) was administered subcutaneously (injection volume 10µl/g body weight). JLK-6 (Calbiochem, 565772) was dissolved in 50% DMSO and 50% H_2O and administered subcutaneously (5mg/kg, 10µl/g). Control mice were injected with vehicle only. DAPT treatment for 48h represents daily injections P3-4 and analysis on P5. DAPT treatment for 96h represents daily injection P2-5 and analysis on P6. DAPT treatment for 3 or 6h represents single injections on P4 or P5. Jag1 peptide (CDDYYYGFGCNKFCRPR) and scrambled peptide (RCGPDCFDNYGRYKYCF; sequences from ref 10; synthesis by Thermo Electron Corporation and Peptide Synthesis Laboratory, London Research Institute, Cancer Research UK) were dissolved at 10 mg/ml in 50% DMSO and 50% H_2O and injected (25 µl/injection) subcutaneously 4 times (0,12,24,36h) for 48 hr treatments, once (0h) for 6h treatments.

Mice and tissues. Wild type mice derived from crossing between male C57Bl6 and female outbred NMRI mice were used for GSI treatment. VE-Cadherin-CreERT2 mice[2], Notch1$^{floxed/floxed}$ mice (obtained from Freddy Ratke[3]) and R26R[4] (obtained from Jackson Laboratories) were all on congenic C57Bl6J background. Dll4+/- mice[5] were maintained on outbred ICR background. Eyes were fixed in 4% parformaldehyde (PFA) for 1 hr (immunohistochemistry) or over night (*in situ* hybridization), rinsed in phosphate buffered saline (PBS) and either directly dissected and stained or dehydrated and stored in 100% methanol at –20°C.

Genomic deletion of Notch 1. Notch1 deletion was induced in VEcad-Cre^{ERT2}/R26R or VEcad-Cre^{ERT2}/Notch1$^{floxed/floxed}$ pups by intragastric injection of 50ng tamoxifen free base (MP Biomedicals, Atlanta) dissolved in sunflower oil at post-natal days (P) 0-4. Littermate control mice were injected with sunflower oil alone. Retinas were collected from P5 pups and fixed in 4% PFA in PBS for evaluation of vascular pattern or in a solution containing 0.2% glutaraldehyde, 5 mM EGTA, 2 mM MgCl2 in PBS, pH 7.3 for assessment of Cre-recombinase activity. Glutaraldehyde-fixed retinas were rinsed three times for 30 min each in a solution containing 2 mM MgCl2, 0.01% DOC, and 0.02% NP-40, in PBS, pH 7.3. The retinas were stained at 37°C in a solution containing 1 mg/ml X-gal (5-bromo-4-chloro-3-indolyl-beta-D-galactopyranoside), 5 mM potassium ferricyanide, 5 mM potassium ferrocyanide, 2 mM MgCl2, 0.01% DOC, and 0.02% NP-40, in PBS, pH 7.3 in order to examine deletion efficiency. Combined LacZ (red) and Isolectin B4-FITC (green) staining was visualized using reflection settings for the 563nm laser on high power micrographs (red signal in fig 2l). TNR mice were generated as described[6].

ROP/OIR model. Pathological eye angiogenesis was induced as described[7], with the modification that 80% oxygen was used during the P7-12 hyperoxia period before return to normoxia during P12-17.

Immunohistochemistry and mRNA in situ hybridization. Isolectin B4 and GFAP staining as well as mRNA in situ hybridization was performed as described[8]. We used rabbit-anti GFP polyclonal antibody (A11122, Molecular Probes, Invitrogen) and monoclonal Rat-anti-mouse Dll4 (1:100, clone 207822, R&D Systems, Abingdon, UK). Activated Notch1 was visualized using rabbit-anti NICD (1:200, ab8925, Abcam, Cambridge, UK) and rabbit-anti cleaved Notch1 (1:50, Val1744, Cell Signaling). For activated Notch1 labeling, pups were perfusion fixed through the

heart, eyes enucleated and fixed in 4%PFA for 1h, retinas dissected and quickly attached to glass slides with the inner-limiting membrane facing down using a thin layer cyanacrylate glue. Subsequently, all neuronal layers were removed with fine tungsten needles, leaving a preparation of the inner-limiting membrane with the full vessel network and associated astrocytes and pericytes on the slides. Immunohistochemistry was performed as above. Bromodeoxyuridine (BrdU) labeling of proliferating cells (2h post-injection) was performed according to according to published protocols[9] allowing combined nuclear staining, BrdU- and isolectin B4-labeling to discriminate between nuclei belonging to endothelial tip- and stalk-cells.

Confocal laser scanning microscopy was performed using Zeiss LSM 510 Meta microscopes (Zeiss, Hertfordshire, UK). Combined in situ hybridization and immunoflourescence labeling was visualized using transmission mode for overview images (grey in situ signal in Suppl Fig S10) or using reflection settings for the 633nm laser on high power micrographs (blue signal in fig 1-3). Images were analyzed in Volocity 3.0.1 (Improvision, Coventry, UK) and compiled using Adobe Photoshop CS 8.0 (Adobe Systems, Uxbridge, UK).

Quantifications. For cell counting experiments, we combined nuclear labeling with endothelial labeling using isolectin BS-I or VE-cadherin. Quantifications were performed at high magnification and resolution, mostly in a confocal microscope to visualize only a limited z-section of the retina to allow for discrimination between endothelial and non-endothelial nuclei.

Tip-cell number: For long-term Notch inhibition experiments, or genetic loss-of-function of dll4, where effects occur across wide zones of the retina, we scored tip cells as blind-ended endothelial protrusions with associated filopodial bursts in areas at the front (20 fields sized 220x294µm; 6 retinas/group for DAPT-treated and control

mice; 40 fields 6-8 retinas/group for dll4 +/- and +/+ mice).

Filopodia protrusions: For the short-term experiments, where effects occur only at the vascular front, we measured the continuous length of endothelial membrane along the leading edge of the growing vascular plexus and counted the filopodia protrusions along this length using ImageJ (Version 1.36b NIH public domain software). We calculated the number of filopodia per 100 um of vessel length from 50 microscopic fields (field size 200x200µm) picked from 6-10 retinas/group for DAPT treatments and from 20 fields of the same size picked from 6 retinas per group for the Jag1/scJag1 treatments. We initially validated the reliability of measurement by repeating the quantification in triplicate on 10 test images. The images for quantification were number coded and quantified in a blinded way. To further validate the quantification method, 30 images from normal retinas unrelated to the experiment were independently quantified by a naïve person, revealing high degree of reproducibility with very similar numbers of filopodia protrusions per membrane length unit at the growing vascular front.

Branchpoints and vessel diameter: To assess the density of the vascular plexus, we quantified the number of branchpoints per area (200x200µm fields, micrographstaken with 20x 0.75 NA lens, 24-32 fields, 6-8 retinas/group for DAPT treated; 22-33 fields; 6 retinas/group for Jag1/scJag1 treated). Using the same micrographs. 10 random vessel diameters were measured on each micrograph (300 vessels; 6-8 retinas/group).

Endothelial cells per vessel length and field: The number of endothelial cell nuclei was counted per 100 µm of vessel length (18 fields, 6 retinas/group for 48h DAPT-treated; 17 fields, 6 retinas/group for 3 or 6h DAPT treated) and vessel length measured per confocal field (250x250x1.2µm, taken with a 40x lens; 7 fields, 6-8

retinas/group for 48h DAPT treated; 17 fields, 6 retinas/group for 3 or 6h DAPT treated).

BrdU-labeled tip and stalk cells: The number of BrdU-positive tip-cells (scored as isolectin BS-I positive cells with extensive filopodia protrusions) was counted on material triple stained for BrdU, isolectin BS-I and DAPI or propidium iodide to determine the location of the BrdU-positive nuclei in relation to other nuclei (e.g stalk cells, pericytes and astrocytes). The analysis was performed when sitting in front of the confocal microscope using the 40x or 63x lens to allow for scanning in z-level to determine that the BrdU positive nuclei truly belonged to a tip-cell. The ratio between BrdU-positive and negative tip-cells was directly compared between control and GSI treated (8-10 retinas/group). The number of BrdU-positive stalk cells was counted and vessel length measured per confocal field (250x250X1.2µm, taken with a 40x lens), and the number of BrdU positive stalk cells was normalized against the total number of endothelial cells/vessel length.

Pdgf-b positive vessel area was calculated on 8-10 retinas/group and the relative levels of pdgf-b mRNA measured by Q-PCR was calculated on 10-11 retinas/group (100% = mean of 11 control Q-PCR measurements).

Mosaic recombination in VEcad-Cre^{ERT2}/Notch1$^{floxed/floxed}$/R26Rmice was analyzed by lacZ staining in combination with isolectin B 4 and TOPRO-3 staining in 139 cells identified in 6 retinas with low degree recombination, of which 43 cells were lacZ positive and 96 cell lacZ negative.

All quantitative data were compiled and analyzed using unpaired two-tailed Student's T-test in Prism 4 (GraphPad software).

Retinal VEGF-A ELISA. Eyes were dissected in ice cold PBS and lysed using a rotor stator in 200 µl lysis buffer containing 1 % NP-40; 0.4 % Na Deoxycholate, 10

mM Tris pH 7. 5, 66 mM EDTA, 150 mM NaCl, supplemented with 4% protease inhibitor (Mammalian Protease Cocktail inhibitor P8340; Sigma-Aldrich). The lysates were centrifuged for 5 min at 2200 rpm and the supernatants were collected. The mouse VEGF-A ELISA kit from R&D Systems, Minneapolis, USA, MMV00, was used to quantify the VEGF-A concentration in the protein lysates.

Gene expression analyses by real-time PCR after DAPT treatment. Eyes were enucleated from mice after 6 hours DAPT or vehicle treatment and were stored in RNA*later* (Qiagen) before and during dissection of retinas. Total retinal RNA was isolated using RNeasy® Mini Kit (Qiagen) according to manufacturer's instructions. First-strand cDNA was synthesized using SuperScript™ III First-Strand Synthesis System for RT-PCR (Invitrogen) with oligo$(dT)_{20}$. 160ng total RNA was used per 20µl reaction volume following manufacturer's recommendations. 6µl of the synthesized cDNA was subsequently used for a 50µl TaqMan assay. Each TaqMan assay was run in duplicates for each RNA sample. Assays were run with TaqMan® 2× Universal Master Mix on ABI Prism 7700 Sequence Detection System with TaqMan® Gene Expression Assays (Applied Biosystems) specific for *Pdgfb* (Mm00440678_m1)), *Nrarp* (Mm00482529_s1), *Dll4* (Mm00444619), *Vegfa* (Mm00437304_m1), *Vegfr1* (Mm00438980_m1), *Vegfr2* (Mm00440099_m1), *Np1* (Mm00435372_m1) and *Slc2a* (Mm00441473_m1). Mouse ACTB (actin, beta) (VIC®/MGB) (Applied Biosystems) was used as an endogenous control to normalize the data.

References

1. Searfoss, G. H. et al. Adipsin, a biomarker of gastrointestinal toxicity mediated by a functional gamma-secretase inhibitor. *J Biol Chem* 278, 46107-46116 (2003).
2. Monvoisin, A. et al. VE-cadherin-CreER(T2) transgenic mouse: A model for

inducible recombination in the endothelium. *Dev Dyn* 235, 3413-3422 (2006).
3. Wolfer, A. et al. Inactivation of Notch1 in immature thymocytes does not perturb CD4 or CD8T cell development. *Nat Immunol* 2, 235-241 (2001).
4. Soriano, P. Generalized lacZ expression with the ROSA26 Cre reporter strain. *Nat. Genet.* 21, 70-71 (1999).
5. Duarte, A. et al. Dosage-sensitive requirement for mouse Dll4 in artery development. *Genes Dev* 18, 2474-2478 (2004).
6. Duncan, A. W. et al. Integration of Notch and Wnt signaling in hematopoietic stem cell maintenance. *Nat Immunol* 6, 314-322 (2005).
7. Smith, L. E. et al. Oxygen-induced retinopathy in the mouse. *Invest Ophthalmol Vis Sci* 35, 101-111 (1994).
8. Gerhardt, H. et al. VEGF guides angiogenic sprouting utilizing endothelial tip-cell filopodia. *J Cell Biol* 161, 1163-1177 (2003).
9. Tkatchenko, A. V. Whole-mount BrdU staining of proliferatijng cells by DNase treatment: application to postnatal mammalian retina. *Biotechniques* 40, 29-30 (2006).
10. Weijzen, S. et al. The notch ligand Jagged-1 is able to induce maturation of monocyte-derived human dendritic cells. *J Immunol* **169**, 4273-4278 (2002).

Legends to Supplementary Figures

Supplement Figure S 1. Notch sparing GSI does not affect retinal angiogenesis.

Isolectin B4 stained retinas, P5 control treated and JLK-6 treated (injected P3 and –4) showing normal vascular development. Note that the control is the same as in Figure 1c.

Supplement Figure S 2. γ-secretase inhibition promotes excessive sprouting angiogenesis in the oxygen induced retinopathy (OIR) model.

Isolectin B4 stained OIR retinas. Overview of control treated P17 retina, **a**, and DAPT treated retina injected P12-16, and sacrificed P17, **b**, shows an increased vascularization of the central area of the retina after DAPT treatment. The avascular areas are outlined in **a** and **b**. **c**, central portion of a vein showing an arterio-venous (A-V) shunt where two arteries feed directly into the vein, and capillary sprouting from the vein into the central area in a control treated retina. Central portion of a DAPT treated retina showing hyper sprouting from the vein, **d**. In particular, note the increased sprouting density from the vein after DAPT treatment, **d**. Peripheral vascular plexus was denser in DAPT treated retina, **f**, compared to control, **e**. The number of capillary enclosed areas was quantified as an indirect measurement of vessel branching. Per 200x field of view there were: 235+/-21 vs. 131+/-9 (mean +/- SEM) capillary enclosed areas, in DAPT and control respectively, t-test $p<0,001$. There was also a reduced formation of epiretinal vascular tufts in DAPT treated retinas as compared to control: DAPT, 165+/-19 vs. 496+/-83, (mean +/- SEM) t-test $p<0,01$.

Supplement Figure S 3. Example of quantification of tip cell proliferation after 6h GSI treatment.

Isolectin B4 (**green**) stained retinas at P5 after 6h DAPT treatment combined with BrdU staining (**red**) and To-Pro-3 nuclear stain (**blue**). Arrow points at BrdU positive tip cell, arrowheads points at BrdU negative tip cells.

Supplement Figure S 4. Down regulation of mRNAs encoding Notch target genes.

Graph showing relative expression of the Notch target gene Nrarp. mRNA from control retinas are set to 100%. Nrarp is down regulated by 70% after 6h DAPT treatment. Error bars represent s.e.m.

Supplement Figure S 5. Functional inhibition of Notch signaling in the developing intestine of P6 mice.

Quantification of goblet cells in the small intestine. An example of PAS and hematoxylin stained paraffin sections from DAPT treated (P2-6) pup. Goblet cells are clearly identified through the red PAS staining. The number of PAS positive cells were normalized against the length of the villus (white line), **a**. Graph showing the number of PAS positive goblet cells per mm of villus length, **b**. There is an 43% increase in the number of goblet cells per length after DAPT treatment, control: 4.6 +/-0.34, DAPT: 6.6 +/-0.38 goblet cells/mm, $p<0.001$. Error bars represent s.e.m.

Supplement Figure S 6. Increased number of *pdgf-b* expressing tip cells at the vascular front of Dll4 +/- mice.

P4 retinas double stained for isolectin (**green)** and *pdgf-b* (mRNA in situ hybridization signal, **blue**) from dll4 +/+ and +/- mice respectively. *pdgf-b* positive tip cells are indicated by white arrows and are more numerous at the vascular front in Dll4 +/- retinas. The lower panel shows only the in situ hybridization signal for *pdgf-b* to facilitate the comparison of the number of *pdgf-b* positive cells at the vascular front in Dll4 +/+ and +/- mice.

Supplement Figure S 7. Visualization of vascular smooth muscle cells and pericytes in Dll4 +/+ and +/- mice.

Double staining for α-smooth muscle actin (ASMA, **red** in a, b) or NG2 (**red** in c, d) and isolectin B4 (**green** in a-d) did not reveal any major changes in vascular smooth muscle cell association with the arteries (**A**) in Dll4 +/-, **c**, **d**, pups compared to littermate controls, **a**, **b**.

Double staining for pericytes (NG2, **red**) and endothelial cells (isolectin B4, **green**) showed normal pericyte numbers and distribution in P4 Dll4 +/- mice at the vascular front, **f**, compared to littermate controls, **e**.

Supplement Figure S 8. Mosaic vascular specific LacZ staining in the retina after tamoxifen treatment of VEcad-Cre^{ERT2}/R26R mice.

Overview of an X-gal stained P5 retina from a VEcad-Cre^{ERT2}/R26R mouse treated with intra gastric injections of Tamoxifen P0-4. LacZ staining (**blue**) is vascular specific and patchy.

Supplement Figure S 9. Normal astrocyte network after GSI treatment.

The astrocytic network (GFAP, **red**) was not primarily affected after 48h GSI treatment (dashed line indicates the vascular front).

Supplement Figure S 10. *vegf-a* mRNA localization, amount, isoforms and VEGF-A protein levels in Dll4+/- and after GSI treatment.

a-f, mRNA *in situ* hybridization for *vegf-a* (black) reveal expression mainly in front of the growing plexus in controls, **a**,**c**,**e**, and after 6h GSI treatment, **d**, but significantly expanded *vegf-a* expression into the peripheral vascular plexus in *Dll4*+/-, **b**, and 48h DAPT-treated, **f**, retinas. Quantitative PCR of *vegf-a* after 6h DAPT treatment reveal a small (10%) but significant increase in *vegf-a* mRNA levels, **g**, while there was no detectable change in another hypoxia-inducible mRNA, *Slc2a1,* **h**. **i**, rt-PCR of retinal *vegf-a* detecting the isoforms 120, 144, 164 and 188 reveal no major changes in relative isoform expression after 48h DAPT treatment (P5). **j**, ELISA quantification of VEGF-A protein levels from lysed retinas show no significant changes in protein levels after 48h DAPT treatment (P5). Error bars represent s.e.m.

Supplement Figure S 11. Schematic model of the role of Dll4/Notch1 signaling in tip cell selection.

A graded distribution of VEGF-A provides an "analogue" tip-cell inducing signal that is received broadly in the endothelial cell population. Some of the VEGF-A-induced cells also respond with upregulated Dll4 expression, which in turn activates Notch1 signaling in neighboring cells to suppress their tip cell phenotype. As a result (A-D conversion), a

limited number of cells become selected as tip cells to guide sprout extension, whereas the remaining cells form the sprout stalks (normal sprouting). When Dll4/Notch1 signaling is inhibited, A-D conversion fails, resulting in the induction of too many tip cells in response to VEGF, which leads to hypersprouting. It is unclear why the Dll4 signal becomes restricted to certain endothelial cells, including but not necessarily limited to tip cells (Fig 2a). We do not favor a classical lateral inhibition scenario, as we did not find a broader expression of Dll4 in Dll4+/- (data not shown) or GSI-treated (data not shown) mice. Genetic restrictions (pre-patterning) or additional signals from the environment need to be considered.

Supplement Figure S 1

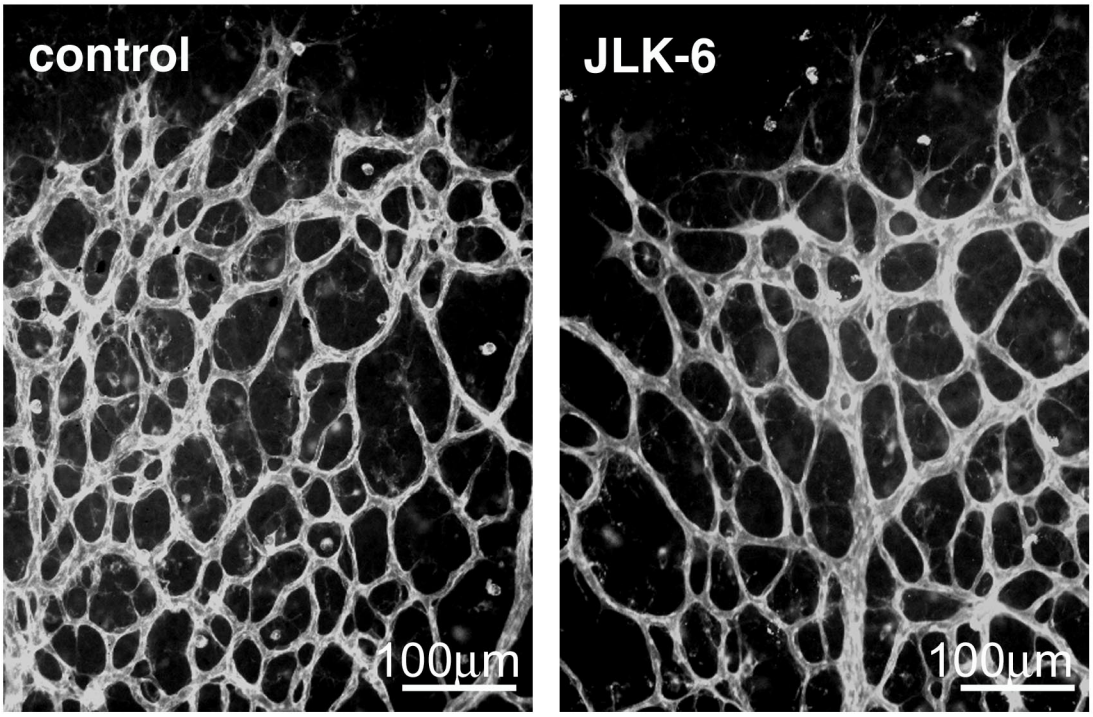

Supplement Figure S 2

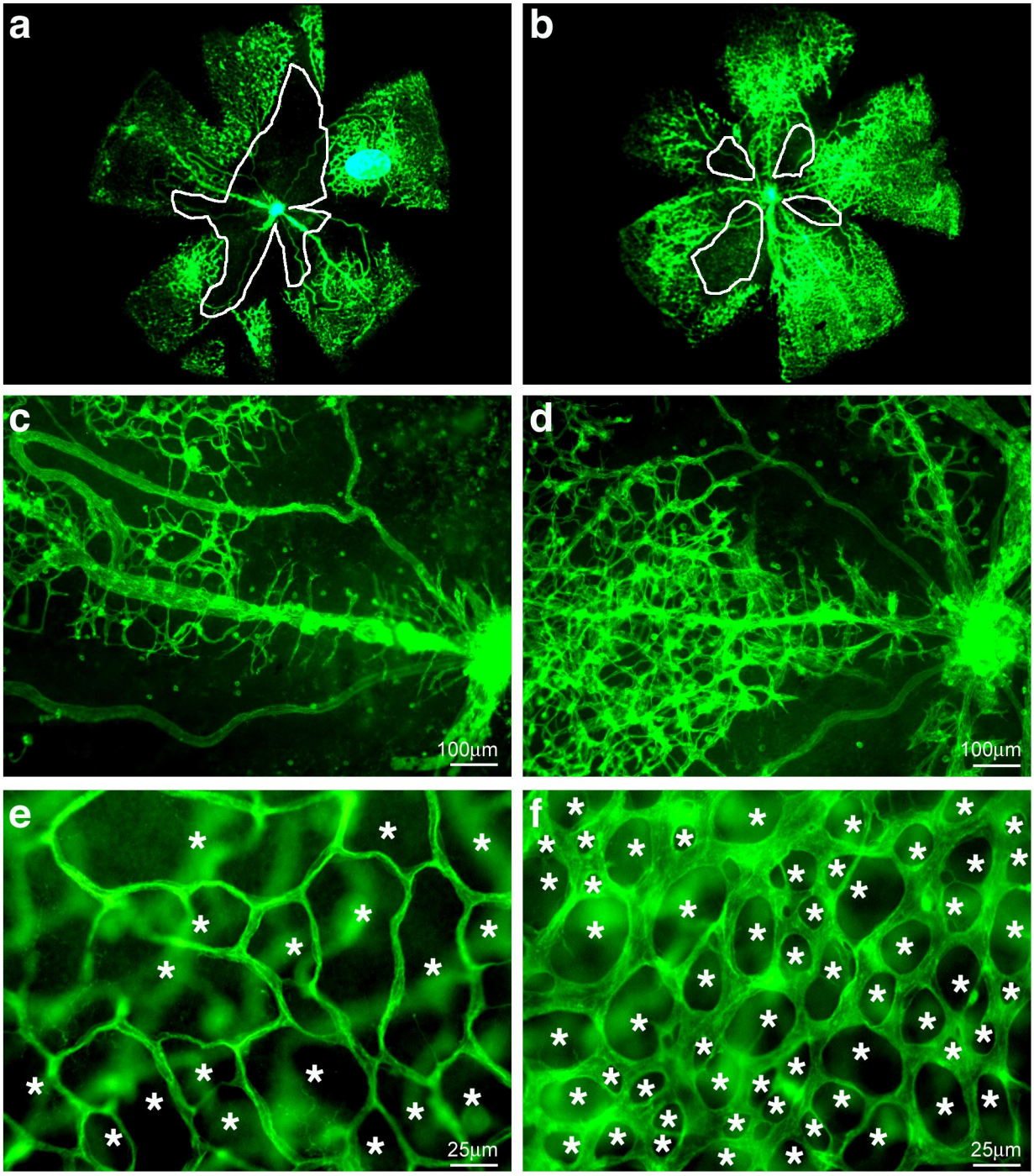

Supplement Figure S 3

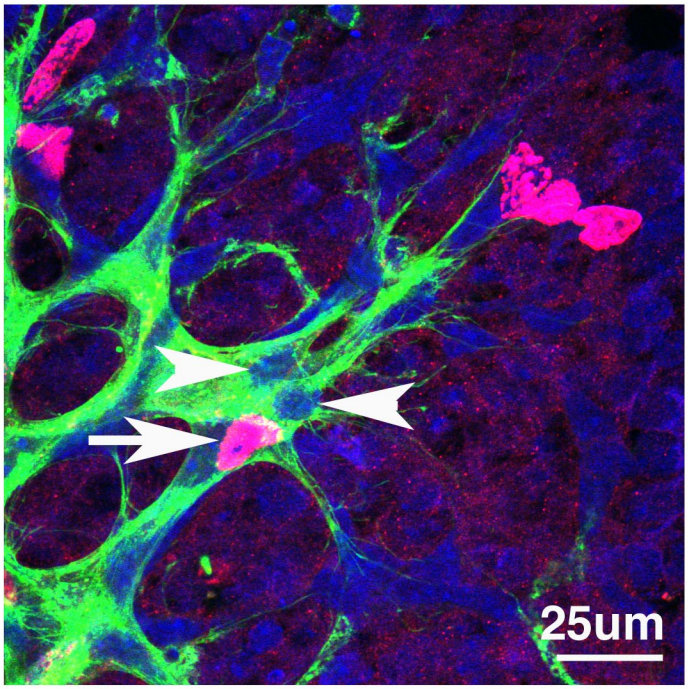

Supplement Figure S 4

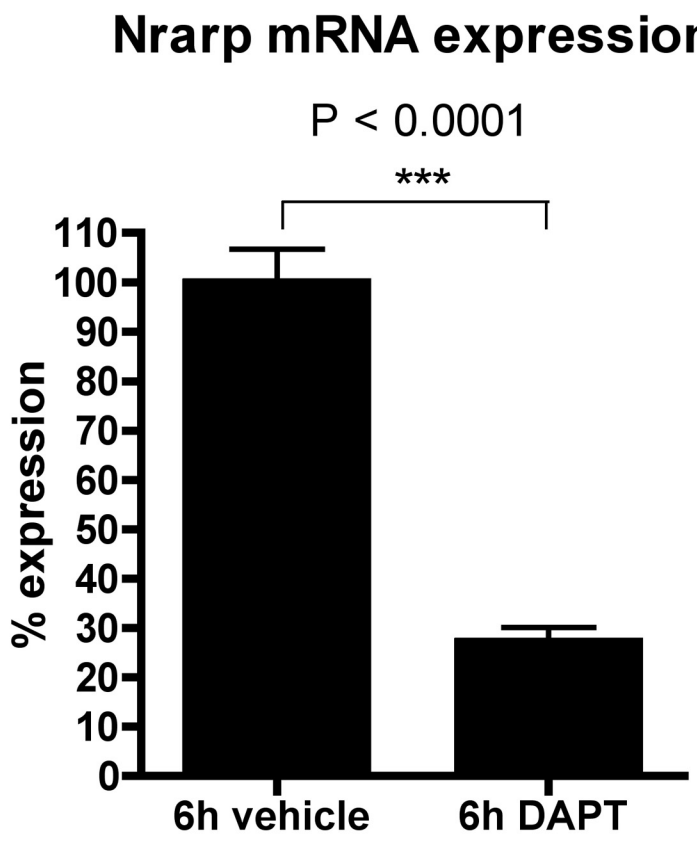

Supplement Figure S 5

a

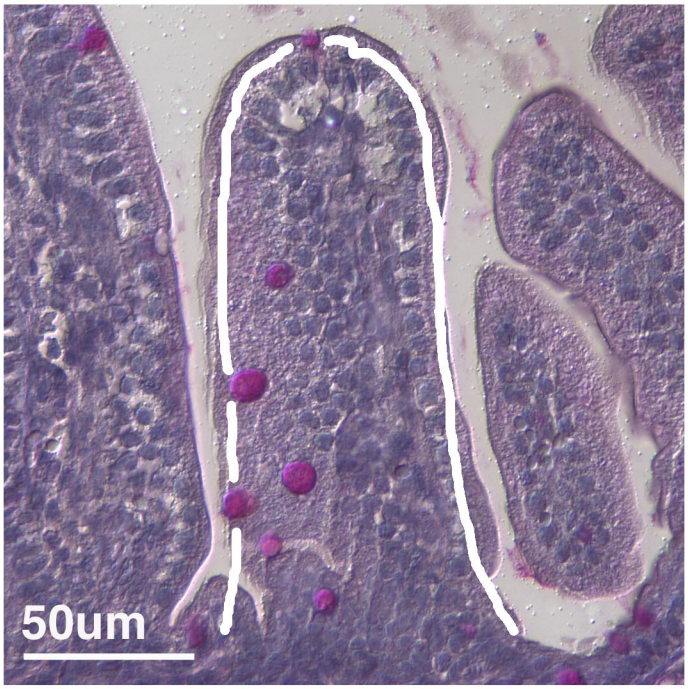

b

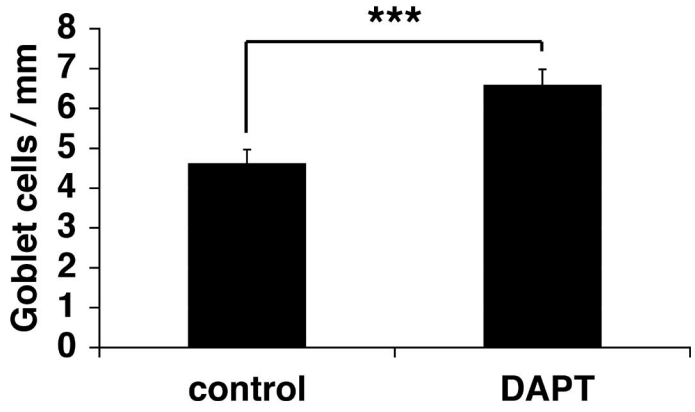

Supplement Figure S 6

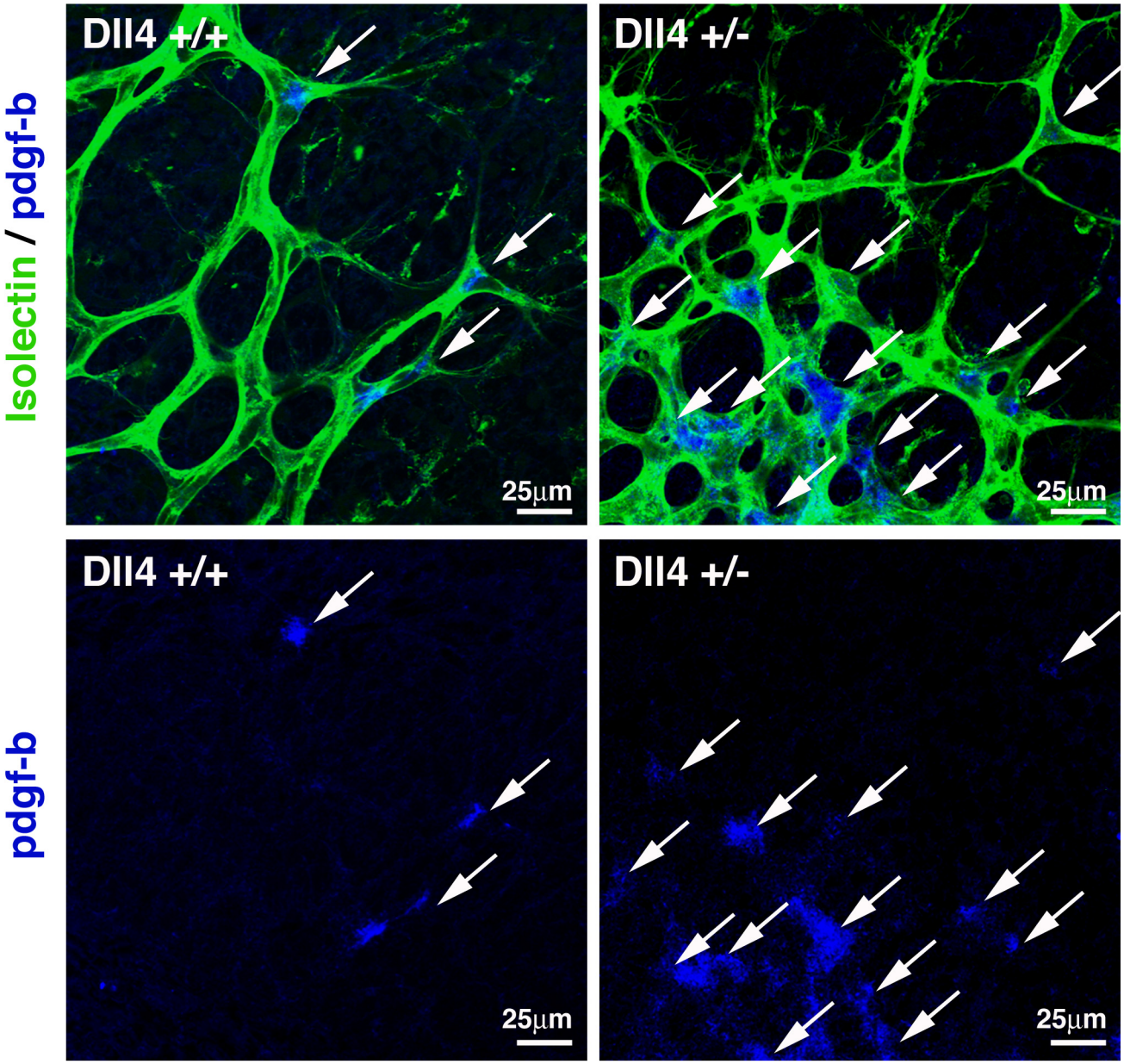

Supplement Figure S 7

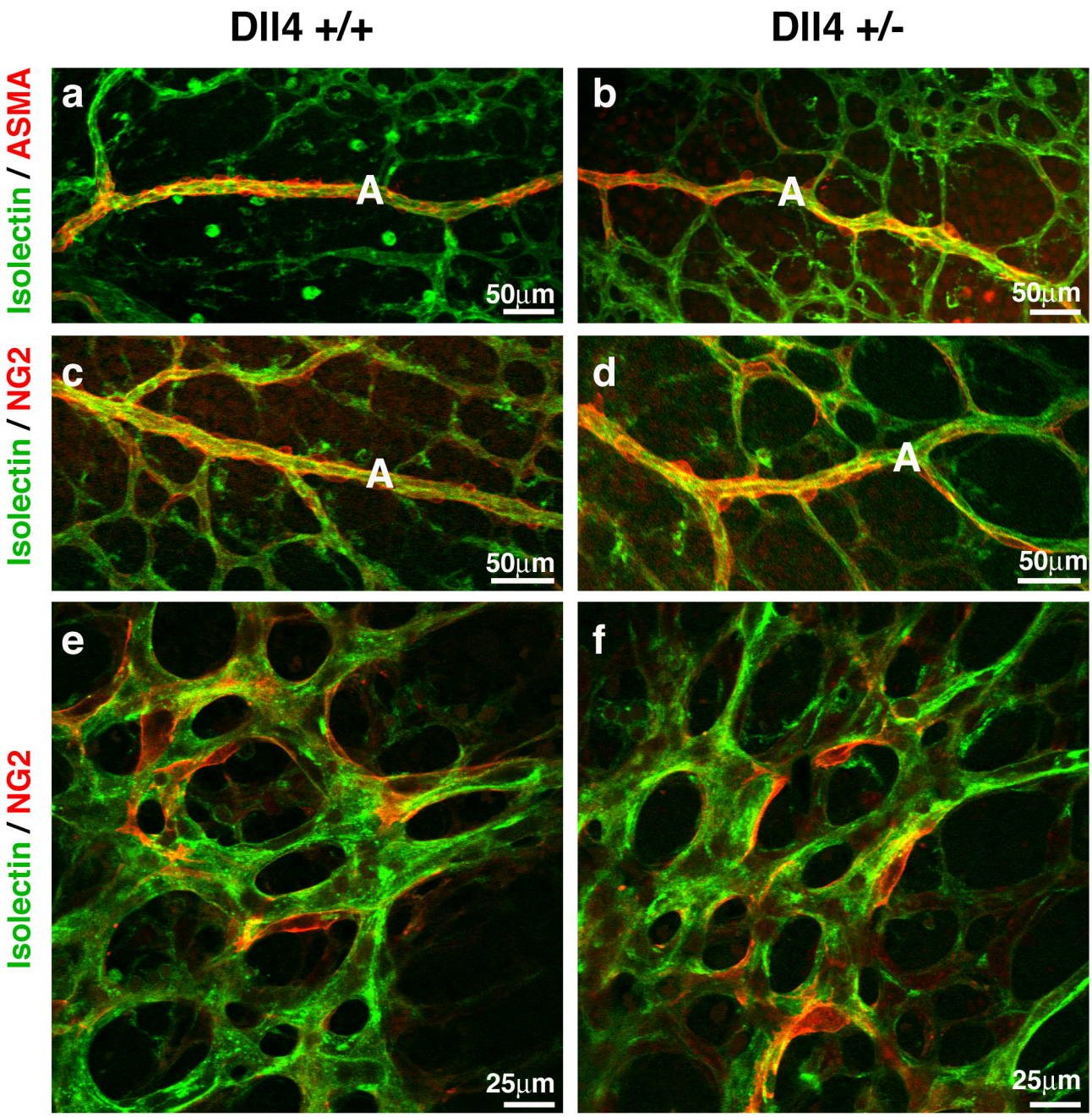

Supplement Figure S 8

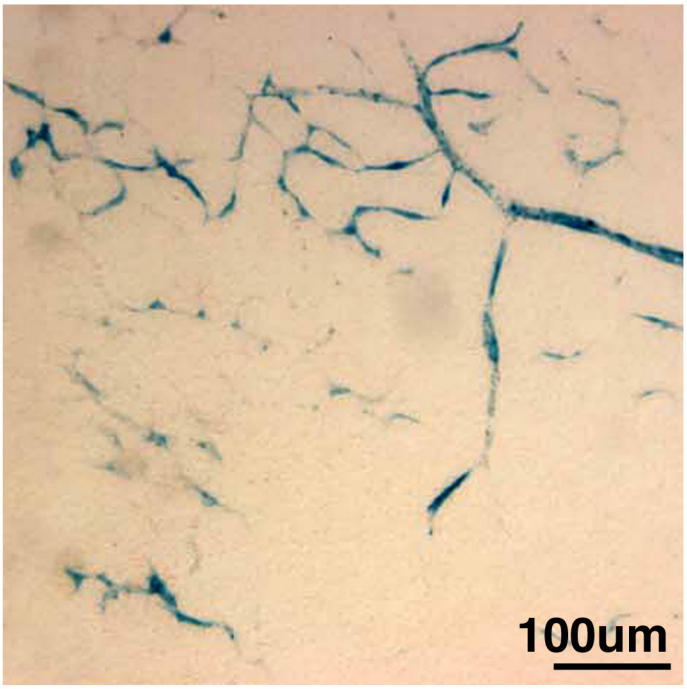

Supplement Figure S 9

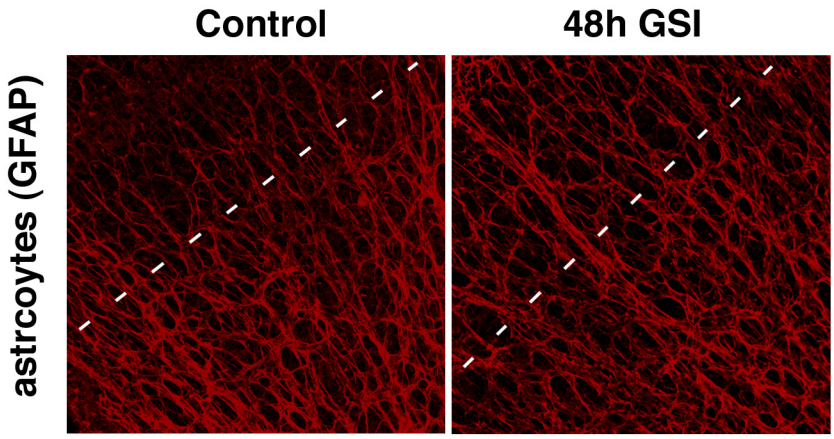

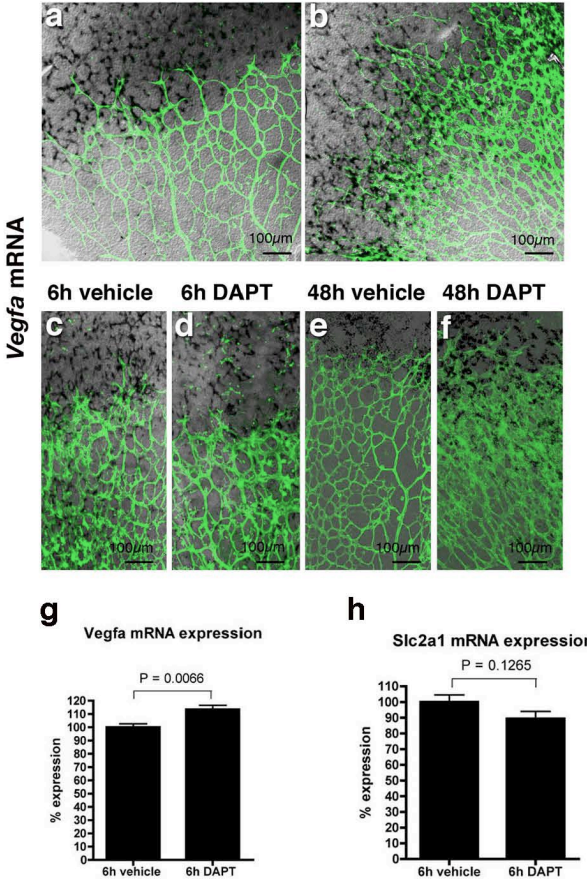
a
b
100μm
100μm
6h vehicle
6h DAPT
48h vehicle
48h DAPT
Vegfa mRNA
c
d
e
f
100μm
100μm
100μm
100μm
g
Vegfa mRNA expression
P = 0.0066
% expression
6h vehicle
6h DAPT
h
Slc2a1 mRNA expression
P = 0.1265
% expression
6h vehicle
6h DAPT

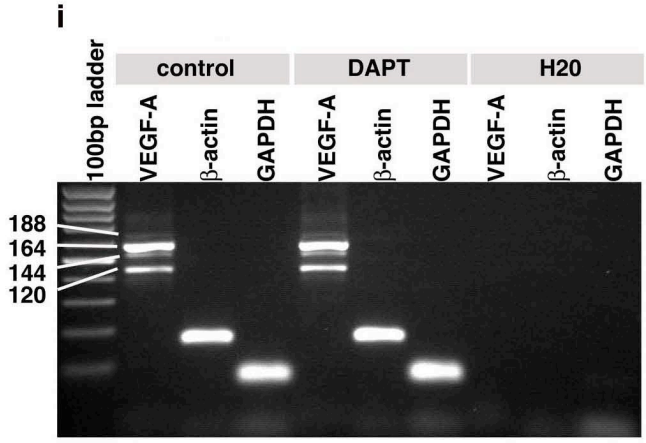
i
100bp ladder
control
DAPT
H20
VEGF-A
β-actin
GAPDH
188
164
144
120

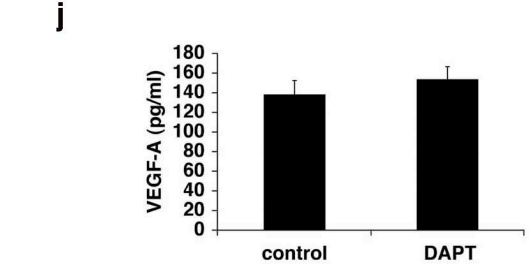
j
VEGF-A (pg/ml)
control
DAPT

Supplement Figure S 11